This article has been accepted for inclusion in a future issue of this journal. Content is final as presented, with the exception of pagination.

Impact of Midpoint STATCOM on Generator Loss of Excitation Protection

Mohamed Elsamahy, *Member, IEEE*, Sherif Omar Faried, *Senior Member, IEEE*, and Tarlochan Sidhu, *Fellow, IEEE*

***Abstract*—This paper explores the impact of a transmission-line midpoint STATCOM on the performance of the generator loss-of-excitation (LOE) protection. In this context, investigations are conducted on a two-hydrogenerator power station for two LOE contingencies, namely, a complete LOE due to a field-winding short circuit and a partial LOE due to a sudden drop in the excitation voltage at different generator loadings. The results of these investigations show that the midpoint STATCOM has adverse impacts on the LOE distance relay in the form of delay time and/or underreach phenomenon. These adverse impacts vary with the generator loading and the LOE mode. The time-domain simulation studies are conducted using PSCAD/EMTDC software.**

***Index Terms*—Generator loss-of-excitation (LOE) protection, generator steady-state stability limit, generator under excitation limiter, generator underexcited capability limit, static synchronous compensator.**

I. Introduction

During the North American blackout on August 14, 2003, misoperation of 13 types of generating units' protective relays was recorded. As a result of these misoperations, around 52 745 MW were lost (290 units mistripped). In addition, the analysis of the major disturbances since 2007 has shown that 12 protection system misoperations, out of 39 occurred during those events, and had been due to the miscoordination between the generation and the transmission protection systems [1]. Reference [1] attributes these misoperations to the fact that the coordination between such protection systems is rarely modeled in dynamic simulations, where it is usually assumed that those protection systems will operate normally and they are coordinated. Recently, the North American Electric Reliability Council (NERC) has demanded from utilities to verify the coordination between generator protection, generator capability, generator control, and transmission-line protection. In this regard, an important issue that must be taken into consideration during such coordination is the presence of flexible ac transmission systems (FACTS) controllers in transmission systems.

Manuscript received February 27, 2013; revised July 12, 2013; accepted September 04, 2013. Paper no. TPWRD-00233-2013.

M. Elsamahy is with the Department of Electrical Power and Energy, Military Technical College, Cairo 1178, Egypt (e-mail: mohamed.elsamahy@usask.ca).

S.O. Faried is with the Power Systems Research Group, University of Saskatchewan, Saskatoon, SK S7N 5A9 Canada (e-mail: sherif.faried@usask.ca).

T.S. Sidhu is with the University of Ontario Institute of Technology, Oshawa, ON L1H 7K4 Canada (e-mail: Tarlochan.Sidhu@uoit.ca).

Color versions of one or more of the figures in this paper are available online at http://ieeexplore.ieee.org.

Digital Object Identifier 10.1109/TPWRD.2013.2281581

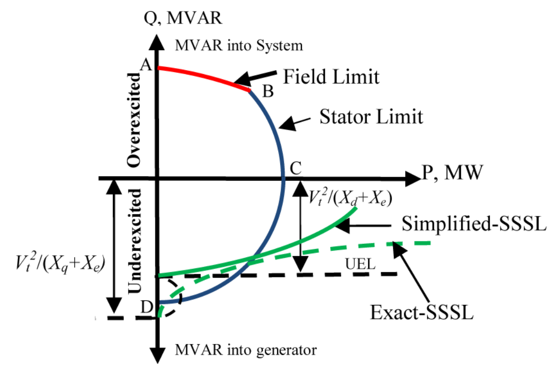

Fig. 1. Capability limits of a salient-pole synchronous machine.

It has been recently reported in [2] and [3] that FACTS controllers have adverse impacts on the performance of the existing transmission-line distance protection relays. The results of these studies show that midpoint shunt FACTS controllers can affect the distance relays with regards to impedance measurement (overreaching/underreaching), phase selection, and operating times. On the other hand, investigations on the impact of FACTS controllers on the performance of generating unit's protective functions are limited to [4] and [5]. These references address the impact of transmission-line midpoint STATCOM on the performance of an existing generating unit's protective relay, namely, the generator distance phase backup protection [Relay (21)]. The results of these investigations show that the midpoint STATCOM has an adverse effect on the performance of Relay (21) as well as on the coordination between such protection and the generator capability limits. An underreaching phenomena as well as a time delay of Relay (21) have also been reported. Virtually, no research work has been reported on the impact of a transmission-line midpoint STATCOM on the coordination between generator loss-of-excitation (LOE) protection and the generator underexcited capability limit. The main contributions of this paper are as follows.

1) It discusses the coordination between the generator LOE protection and the generator underexcited thermal capability limit.
2) It investigates the impact of the STATCOM on such coordination through several time-domain simulation studies for different LOE contingencies and generator loadings. These studies provide accurate evaluations of Relay (40) performance through monitoring the dynamic behavior of the impedance trajectory measured by the relay with the absence and presence of a midpoint STATCOM.
3) It evaluates the impact of the STATCOM during the LOE on the healthy parallel generator.

II. Considerations During LOE for Multigenerators on the Same Bus

A. Steady-State Underexcited Capability Limit

Fig. 1 shows the steady-state capability limits for a salient-pole synchronous machine. Salient pole rotors have negligible end core region losses. Therefore, the generator underexcited capability (GUEC) limit is determined by the stator winding current limit which extends as a continuous arc from B to D. The GUEC (the leading VAR limit) is represented by the portion of the arc from C to D [6], [7].

B. Steady-State Stability Limit

The steady-state stability limit (SSSL) indicates how far the generator can operate in the leading power factor or the underexcited region of the generator capability curve during normal mode of operation. More specific, SSSL is used in coordination studies to adjust the generator underexcitation limiters (UEL) as will be discussed in Section II-D.

The exact SSSL of a salient-pole generator, shown in Fig. 1, is a nonlinear characteristic. It is obtained by differentiating the generator power-angle equation

$$P = \frac{\mathrm{EV}}{X_d + X_e}\sin\delta + \frac{V^2}{2}\left(\frac{1}{X_q + X_e} - \frac{1}{X_d + X_e}\right)\sin 2\delta \tag{1}$$

and solving for the angle $\delta_{\max}$ at which the maximum power occurs

$$\cos\delta_{\max} = 0.25\left\{\frac{-E\,(X_q+X_e)}{V\,(X_d-X_q)} + \sqrt{\left[\frac{E\,(X_q+X_e)}{V\,(X_d-X_q)}\right]^2 + 8}\right\}. \tag{2}$$

In (1) and (2), E, X_d, X_q, X_e, V, and δ are, respectively, the generator excitation voltage, the direct- and quadrature-axes synchronous reactances, the system external reactance, the infinite-bus voltage, and the generator load angle. The locus of the SSSL is drawn by varying the generator excitation voltage E in small increments, finding $\delta_{\max}$ from (2) and, finally, the corresponding P and Q from (1) and (3)

$$Q = \frac{EV}{X_d + X_e}\cos\delta - \frac{V^2}{2\,(X_d + X_e)\,(X_d + X_e)} \times \{(X_d + X_q + 2X_e) - (X_d - X_q)\cos 2\delta\}. \tag{3}$$

However, the exact SSSL locus for a salient-pole generator is asymptotic to the corresponding locus of a round rotor generator [8]–[10]. Therefore, for simplicity, a simplified-SSSL graphical representation is usually used where the effect of saliency is neglected $(X_d = X_q)$ [1], [11]. This simplified SSSL characteristic, shown in Fig. 1, is plotted as part of a circle with a center C_s and a radius R_s given by

$$C_s = 0,\ \frac{V_t^2}{2}\left(\frac{1}{X_e} - \frac{1}{X_d}\right)$$

$$R_s = \frac{V_t^2}{2}\left(\frac{1}{X_e} + \frac{1}{X_d}\right) \tag{4}$$

where V_t is the generator terminal voltage.

C. Short-Time Overloading Thermal Capability

System voltage drops, due to switching manipulations or faults, cause system high reactive power requirements. In order to satisfy such requirements, the generator field and armature windings are allowed for short-time overloading levels. The higher current magnitudes enable shorter periods of time, and the lower current magnitudes are allowed for longer periods of time. This behavior is defined by IEEE/ANSI C50.13 and C50.13 [12].

D. Underexcitation Limiter

The generator underexcitation limiter (UEL) is set to avoid the excitation decreasing over the stator-end region heating limit. The UEL characteristic may be represented by a single or multi linear segments or by a curve. Typically, the UEL characteristic is set based to 80%–85% of the most limiting of two conditions: 1) the SSSL or 2) the GUEC with minimum time delay. Some limiters do not have an intentional time delay [13], [14].

E. LOE Protection (Relay (40))

A negative offset mho distance relay with two protective zones is widely used within the industry to provide high-speed detection of generator LOE conditions as shown in Fig. 2(a). In the investigations reported in this paper, such a relay is designated as Relay (40 (or R_{40}) and is typically set as follows [1], [14], [15]: Both Zone 1 and Zone 2 have a negative offset that is equal to 50% of the direct-axis transient reactance $(X_d^{/})$. Zone 1 is set at 1.0 p.u. (generator base); this element detects an LOE during high loading conditions. A short time delay of 0.1 s is allowed to prevent misoperations during switching transients. Zone 2 is set equal to the direct-axis synchronous reactance. This element detects LOE during light loading conditions. A time delay of 0.5 s is allowed to prevent misoperations during power swings. An undervoltage supervising element, designated as UV, is set to pickup at 80%–90% of the generator-rated voltage with a time delay of 0.25–1.0 s.

F. Coordination of Relay (40) with GUEC, UEL, AND SSSL

GUEC (Fig. 1) is usually plotted on a P–Q (MW–MVAR) diagram. On the other hand, Relay (40)'s characteristic is typically displayed on a resistance-reactance (R–X) diagram. To coordinate GUEC with Relay (40), it is necessary to convert the GUEC to an R–X plot. Fig. 2(b) illustrates this conversion where the current-transformer (CT) and the voltage-transformer (VT) ratio $(\mathrm{R_c}/\mathrm{R_v})$ converts primary ohms to secondary quantities that are set within the relay, and kilovolts (kV) is the generator-rated voltage [1], [15].

G. Midpoint STATCOM in Transmission Lines

A midpoint STATCOM regulates the transmission-line voltage at the point of connection by means of electronic processing (pulsewidth-modulation-based switching scheme)

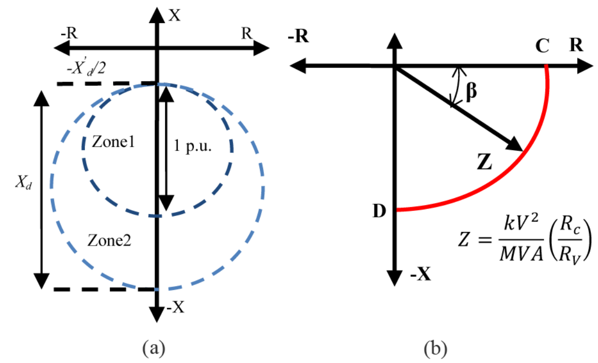

Fig. 2. (a) Negative offset loss of excitation relay [Relay (40)] with two protective zones. (b) Transformation of GUEC, UEL, and SSSL form the P–Q plot to the R–X plot.

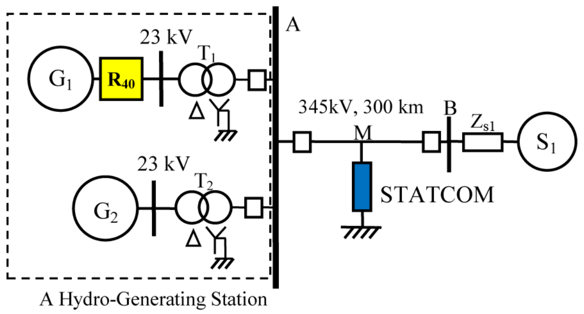

Fig. 3. System under study.

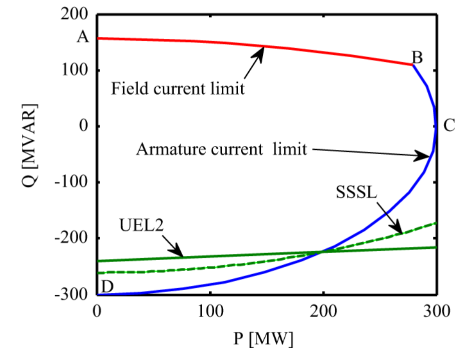

Fig. 4. Capability limits of the hydrogenerators under study.

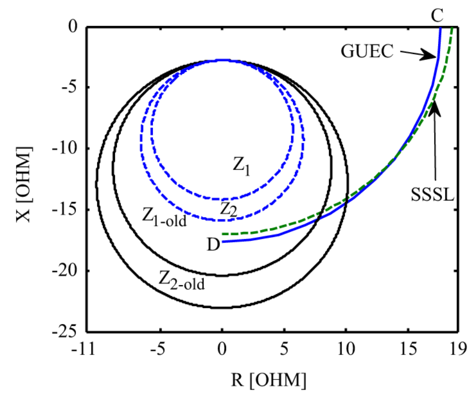

Fig. 5. Relay (40) characteristic of G_1.

of the voltage and current waveforms in a voltage-source converter (VSC), which is controlled by varying the modulation index. In addition, the dc bus voltage of the VSC must be maintained within a prespecified range by implementing a proportional-integral controller [16], [17]. Therefore, the transient responses of the midpoint STATCOM controls during faults cause the impedance trajectory seen by Relay (40) to take longer to converge to a new steady-state value. This results in delaying the operating time of the relay as will be demonstrated in Section III.

III. Performance of Relay (40) With the Presence of a Transmission-Line Midpoint STATCOM

A. System Under Study

The system used in the investigations of this paper is shown in Fig. 3. It consists of a hydro-generating station (comprises two identical generators) connected via two step-up transformers to a large system through a 345 kV, 300 km transmission line. A STATCOM is connected to the transmission line midpoint for the purpose of improving its voltage profile and increasing its power transfer capability. The data of the hydro-generator are taken from [4] and its capability limits are plotted in Fig. 4. The system data are given in Appendix A. Dynamic simulation studies on this test system have been conducted using the PSCAD/EMTDC software [18].

It worth mentioning that during the LOE contingencies considered in this paper (sustained complete LOE and sustained partial LOE), it is assumed that the UEL of G_1 and the OEL of G_2 are disabled. Such an assumption is due to the fact that the contingencies duration is outside their permissible control time. These are discussed in details through the transient time responses presented in Section III-B. Furthermore, regarding the UEL of G_1, a type UEL2 straight-line normalized characteristic of 86% of SSSL (the most limiting as shown in Fig. 4) is plotted in all of the following figures, in order to highlight the problem under investigation.

Another point worth highlighting is, with the current setting of Relay (40) of G_1, it was found that such a setting restricts the GUEC. Therefore, to ensure the coordination between Relay (40) and GUEC during the investigations, the setting of Relay (40) is revised (reduced to 90% of the GUEC in R–X plane), as shown in Fig. 5. Moreover, the undervoltage (UV) supervising element of Relay (40) is set in accordance with the recommendation of [14] and [15]. Such a recommendation states that "for two or more parallel generators at the same bus, it is recommended that the dropout setting of the UV element should be set to pick up at 87%".

B. Simulation Results

In the studies conducted this paper, the performance of Relay (40) of G_1 is examined in accordance with the recommendations highlighted in [1], [15]. Such recommendations state that "a sufficient number of extensive dynamic studies must be performed to determine the worst loading condition for the coordination with the LOE protection; in addition, an attention should be paid for partial loss of excitation during light loading which results in prolonged operation in the underexcited region". Therefore,

TABLE I
SELECTED CASES FOR INVESTIGATING THE PERFORMANCE OF RELAY (40)

	Case	Loading (p.u. of rated generator MVA)	LOE mode
Heavy loadings	1	P = 0.93, Q = 0.36 (point B in Fig. 4), δ_{G1} = 36.45^0, θ_{VA} = 30.79^0, θ_{VM} = 14.61^0, θ_{VB} = 0.	$E_F = 0$
	2	P = 0.93, Q = 0.36 (point B in Fig. 4)	E_F = 0.4 p.u.
Light loadings	3	P = 0.3, Q = -0.11	$E_F = 0$
	4		E_F = 0.4 p.u.

TABLE II
PERFORMANCE OF RELAY (40) DURING LOE MODES WITH THE PRESENCE OF STATCOM (TRIPPED ELEMENTS ARE BOLD UNDERLINED)

Loading (p.u. of rated generator MVA)	E_{F1}, p.u.	Delay time (seconds)		
		UV	Zone1	Zone2
$P_g = 0.93$, $Q_g = 0.36$	0	2.317	**5.4**	5.36
	0.2	2.92	**6.818**	6.786
	0.4	3.83	**9.55**	9.5
$P_g = 0.3$, $Q_g = -0.11$	0	5.216	14.66	**12.74**
	0.2	7.26	25.2	**21.69**
	0.4	14.93	UR	

different LOE contingencies are considered; namely, a complete LOE ($E_{F1} = 0$) due to field short circuit and partial LOE ($E_{F1} = 0.2$ p.u. and 0.4 p.u.) due to sudden drop of the excitation supply after 5 s of starting the simulation time. These LOE contingencies are examined at different generator loading conditions. Due to space limitations, the selected cases shown in Table I will be presented and discussed to evaluate the impact of STATCOM on the performance of Relay (40), while the remaining results are summarized in Table II. The operation of the generator circuit breaker during all case studies was not allowed after Relay (40) tripping in order to obtain the time at which the generator loses synchronism.

1) Transient Time Responses of Generators 1 and 2 During Case 1: Fig. 6 shows generator 1 real power (P_{g1}) transient time responses during Case 1. It can be seen from this figure that due to the LOE at $t = 5$ s, the generator real power decreases and averages around 0.041 in both cases of presence and absence of a midpoint STATCOM. It can also be seen from the same figure that the presence of the midpoint STATCOM extends the time at which G_1 loses synchronism. This is due to the fact that maintaining the transmission line midpoint voltage constant is equivalent to a virtual reduction in transmission line inductive reactance. In other words, the generator is connected in such a case to a "relatively" stiff network.

Fig. 7 shows generator 1 terminal voltage (V_{T1}) and reactive power (Q_1) transient time responses during Case 1 with the absence of the STATCOM. As a result of the loss of excitation (the collapse of E_{F1} to 0), V_{T1} starts to decrease and falls below the UV element threshold at which it picks-up at 7.3 s (after 0.9 s delay time). Similarly, during the same period, Q_1 starts to decrease and falls below the UEL level at which Relay (40) issues a trip signal at 9.07 s.

The impact of the LOE of G_1 in the absence of the midpoint STATCOM on G_2 armature and field currents is shown in Fig. 8. It can be seen from this figure that the field and armature

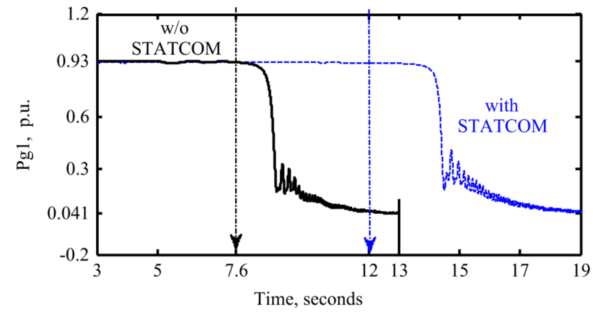

Fig. 6. Generator 1 real power during Case 1 without and with a midpoint STATCOM.

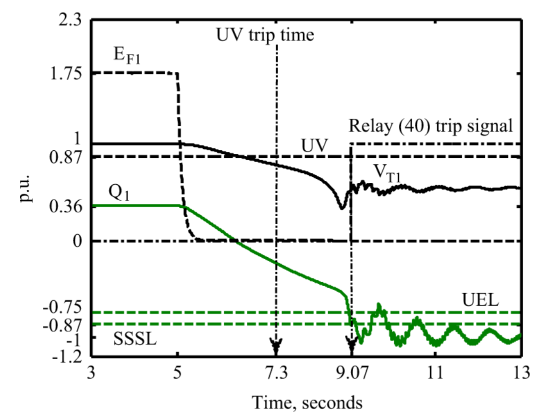

Fig. 7. Generator 1 terminal and excitation voltages, reactive power, UEL, UV element and Relay (40) trip signal during Case 1 without a midpoint STATCOM.

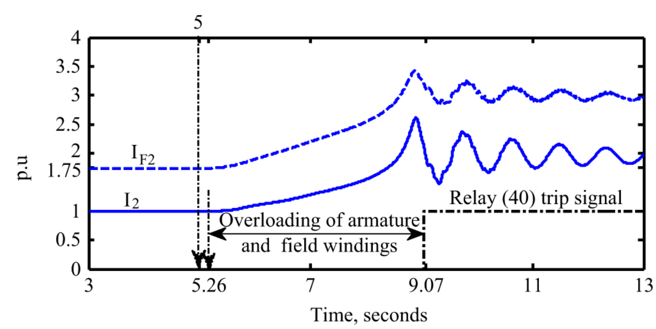

Fig. 8. Overloading of Generator 2 armature and field windings during Case 1 without a midpoint STATCOM.

windings of G_2 suffer overloading for 3.81 s until Relay (40) trips at 9.07 s. This overloading is due to the fact that G_2 is participating in supplying the reactive power absorbed by G_1. During this period, field and armature currents (I_{F2} and I_2) reach levels of 2 and 2.5 p.u., respectively.

Fig. 9 shows V_{T1} and Q_1 transient time responses in the presence of the midpoint STATCOM. In addition, the reactive power supplied by the midpoint STATCOM ($Q_{STATCOM}$) as well as the midpoint voltage (V_M) transient time responses are shown in Fig. 10. It can be seen from Fig. 9 that the STATCOM increases the pickup time of the UV element to 9.62 s. After this time, Q_1 continues to decrease until it goes below the levels of the UEL and the SSSL at which Relay (40) issues a trip signal at 14.47 s. The comparison between Figs. 7 and 9 shows that with

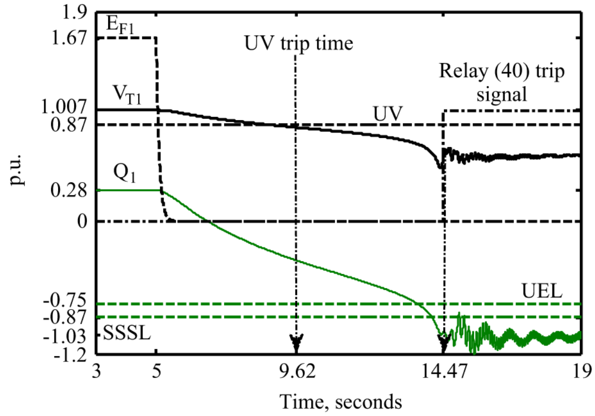

Fig. 9. Generator 1 terminal and excitation voltages, reactive power, UEL, UV element, and Relay (40) trip signal during Case 1 with a midpoint STATCOM.

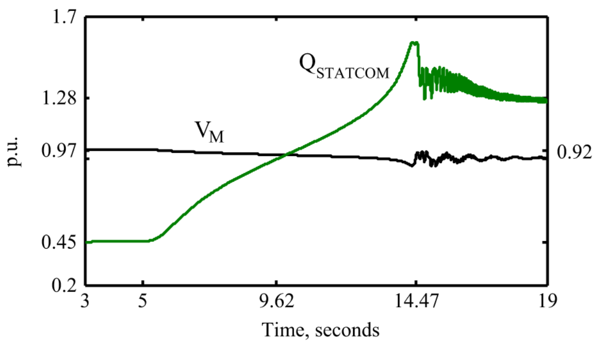

Fig. 10. Reactive power supplied by the midpoint STATCOM and the bus midpoint voltage during Case 1 with the midpoint STATCOM being enabled.

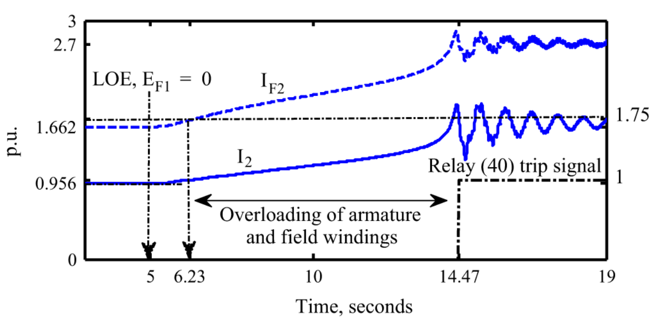

Fig. 11. Overloading of generator 2 armature and field windings during Case 1 with a midpoint STATCOM.

STATCOM in service, the operation of G_1 in the underexcited region during the LOE is extended for 5.4 s.

Fig. 11 shows the impact of the STATCOM during the LOE on generator 2 field and armature currents. The comparison between Figs. 8 and 11 reveals that STATCOM reduces the overloading level of G_2 through its participation in supplying reactive power to G_1. Nevertheless, the comparison shows also that the overloading period is increased by 8.24 s until Relay (40) trips at 14.47 s.

2) Impedance Seen by Relay (40) During Case 1: Fig. 12 depicts the impedance trajectories (A and B) measured by Relay (40) in the absence and presence of the midpoint STATCOM. These trajectories start at $(17.711, 5.438)$ Ω and $(16.572, 6.459)$ Ω without/with the STATCOM, respectively.

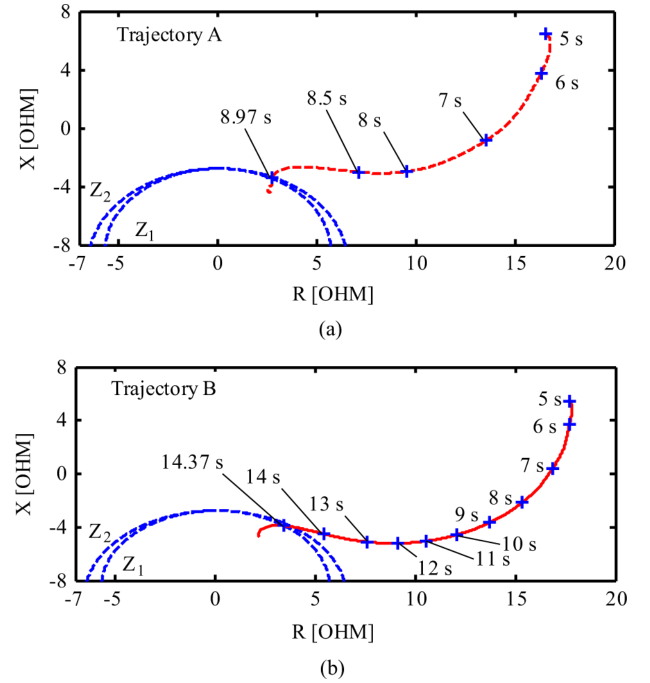

Fig. 12. Impedance trajectory measured by Relay (40) of generator 1 during Case 1: (a) without a STATCOM, (b) with a STATCOM.

Comparing the two trajectories shows that the presence of the STATCOM starts to slow down trajectory B after 6 s of the simulation time. As a result, it takes 14.37 s for trajectory B to penetrate zone 1, while trajectory A penetrates zone 1 at 8.97 s. Finally, Relay (40) trips by zone 1 (after its timer of 0.1 s is timed out) at $\mathrm{t} = 9.07$ s and $\mathrm{t} = 14.47$ s for trajectories A and B without/with STATOM, respectively, as shown in Figs. 7 and 9 .

3) Transient Time Responses of Generators 1 and 2 and Relay (40) Trajectory During Case 2: This case explores the impact of a partial LOE on Relay (40) and its results, illustrated in Figs. 13–15, are compared with those of Case 1.

Such a comparison reveals that generally the results and conclusions of Cases 1 and 2 are very similar except, as it should be expected, the impact of a partial LOE on Relay (40 and G_2 field and armature currents is less severe than that of a complete LOE. In other words, Relay (40) trips at 9.55 s and 19.1 s for Case 2 in the absence and presence of a midpoint STATCOM, respectively, compared to the corresponding values for Case 1 of 9.07 s and 14.47 s. Moreover, the maximum values of G_2 field and armature currents in Case 2 are less than those of Case 1.

4) Transient Time Responses of Generators 1 and 2 During Case 3: This case explores the impact of a light generator loading on Relay (40) during LOE and its results, illustrated in Figs. 16–19, are compared with those of Case 1. The comparison between Figs. 17 and 7 and 9 shows that, the LOE at light loading causes Relay (40) to take longer times for tripping. Moreover, the comparison between Figs. 8 and 18 shows that, at light loading, the LOE does not cause overloading of the G_2 field and armature currents.

5) Impedance Seen by Relay (40) of Generator 1 During Case 3: Fig. 19 depicts the impedance trajectories (A and B) mea-

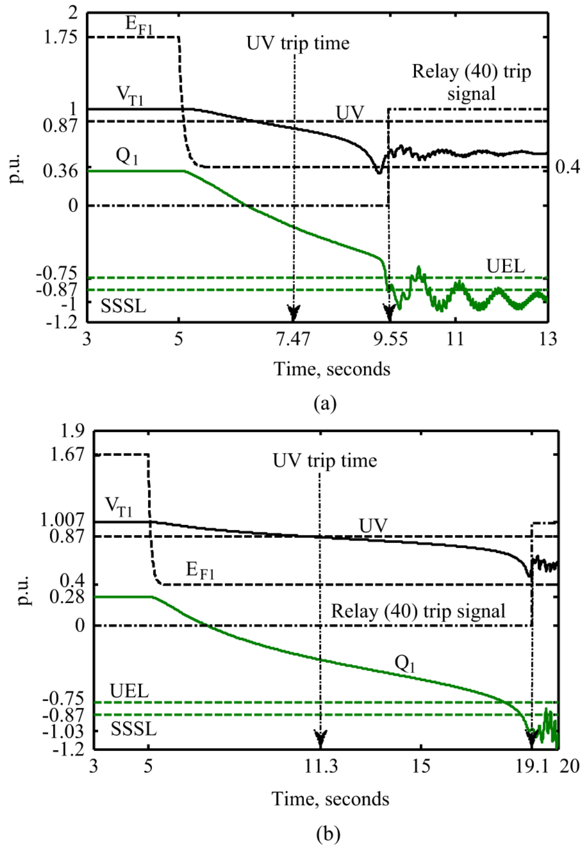

Fig. 13. Generator 1 terminal and excitation voltages, reactive power, UEL, UV element and Relay (40) trip signal during Case 2: (a) without a midpoint STATCOM and (b) with a midpoint STATCOM.

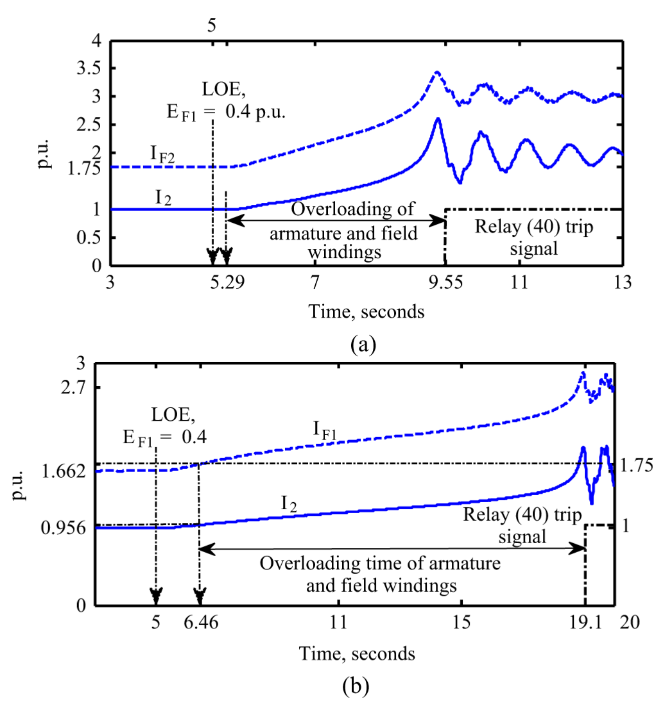

Fig. 14. Generator 2 armature and field currents during Case 2: (a) without a midpoint STATCOM and (b) with a midpoint STATCOM.

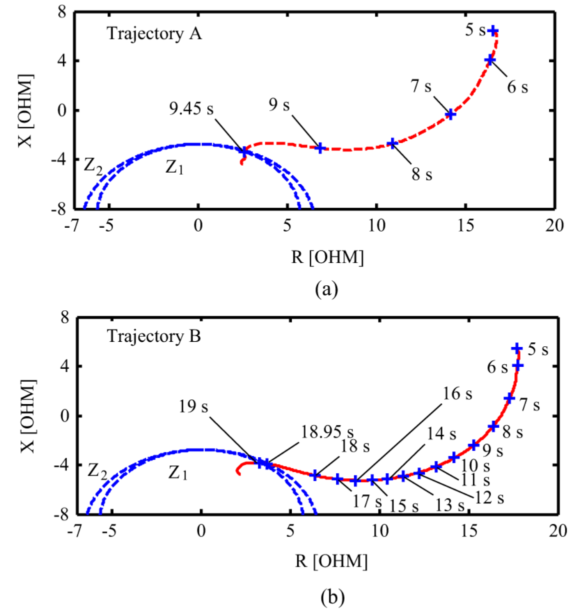

Fig. 15. Impedance trajectory measured by Relay (40) of generator 1 during Case 2: (a) without STATCOM, impedance trajectory starts at $(17.711, 5.438)$ Ω and (b) with STATCOM, impedance trajectory starts at $(16.572, 6.459)$ Ω.

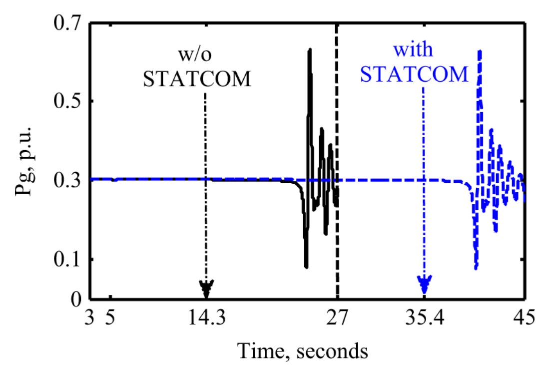

Fig. 16. Generator 1 real power during Case 3 without and with a midpoint STATCOM.

sured by Relay (40) in the absence and presence of the midpoint STATCOM. These trajectories start at $(50.94, -19.27)$ Ω and $(56.79, -11.67)$ Ω without/with STATCOM, respectively. Comparing the two trajectories shows that the presence of the STATCOM starts to slow down trajectory B at 7 s of the simulation time. As a result, it takes 34.86 s and 30.34 s for trajectory B to penetrate Zones 1 and 2, while it takes 20.2 s and 17.6 s for trajectory A to penetrate Zones 1 and 2, respectively. Finally, Relay (40) trips by zone 2 (after its timer of 0.5 s is timed out) at $t = 18.1$ s and $t = 30.84$ s for trajectories A and B without/with STATOM.

6) Transient Time Responses of Generators 1 During Case 4: Fig. 20 shows V_{T1} and Q_1 transient time responses during Case 4 with the presence of the midpoint STATCOM. As can be seen from this figure, the operation of the UV element is delayed until it picks up at 30.11 s. In the meantime, Q_1 continues to decrease and crosses the UEL level at $t = 85.2$ s ($Q_1 = -0.77$ p.u). Such a decrease in Q_1 continues until the end of the simulation time of 14.8 s. This is compatible with the UEL assumption made in Section III. No trip signal is issued by Relay (40).

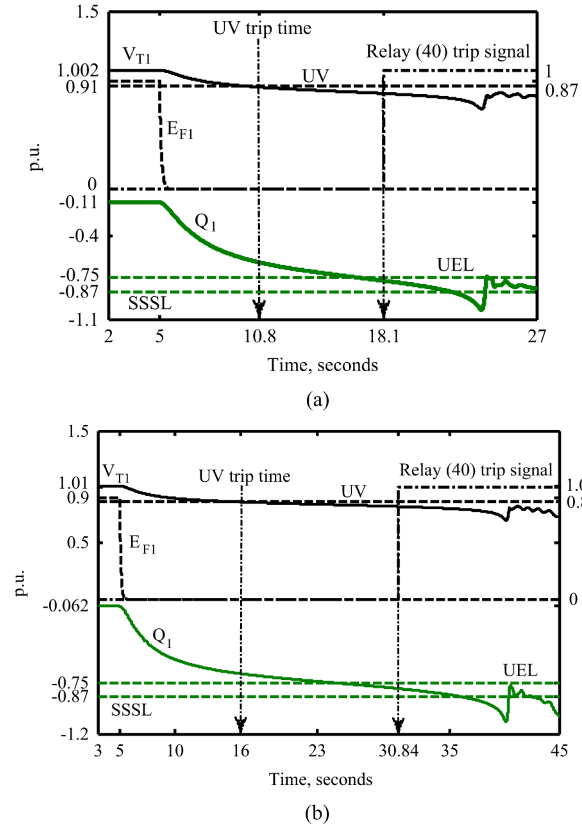

Fig. 17. Generator 1 terminal and excitation voltages, reactive power, UEL, UV element and Relay (40) trip signal during Case 3: (a) without a midpoint STATCOM and (b) with a midpoint STATCOM.

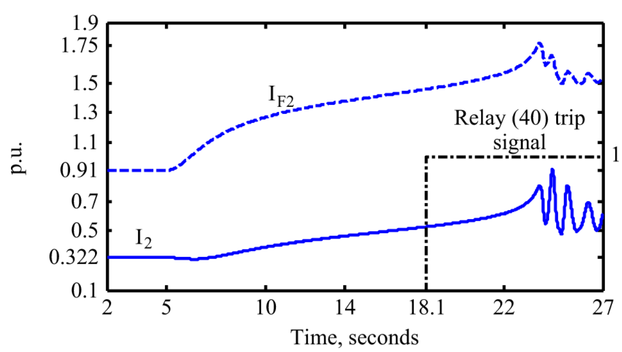

Fig. 18. Generator 2 armature and field currents during Case 3 without a midpoint STATCOM.

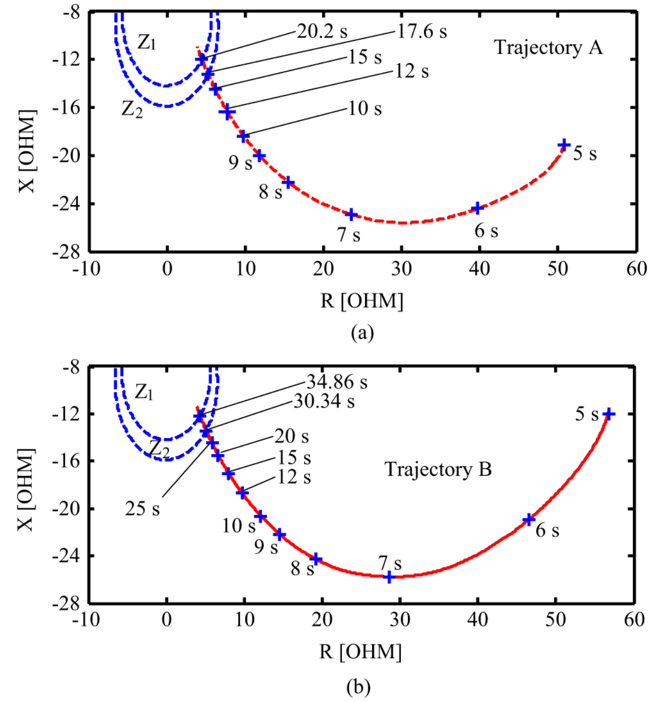

Fig. 19. Impedance trajectory measured by Relay (40) of generator 1 during Case 3: (a) without a STATCOM and (b) with a STATCOM.

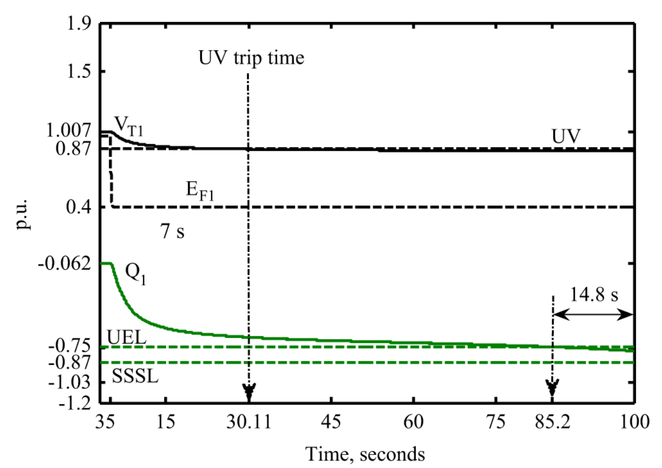

Fig. 20. Generator 1 terminal and excitation voltages and reactive power during Case 4 with a midpoint STATCOM.

7) Impedance Seen by Relay (40) of Generator 1 During Case 4: Fig. 21 depicts the impedance trajectories (A and B) measured by Relay (40) during Case 4 in the absence and presence of the midpoint STATCOM. These trajectories start at $(50.94, -19.27)\ \Omega$ and $(56.79, -11.67)\ \Omega$ without/with STATCOM, respectively. It can be seen from Fig. 21(b), that the impedance trajectory B starts to slow down dramatically at 10 s and after more than 100 s of simulation time it has not yet penetrated the relay characteristic. In other words, the presence of the STATCOM causes Relay (40) to underreach. This is the worst impact obtained during the investigations of this paper. In this regard, Relay (40) can "only" overcome the adverse impact STATCOM if it is set to the original setting shown in Fig. 5. More specific, with the presence of the STATCOM, Relay (40) setting should encroach GUEC in order to detect an LOE condition as shown in Fig. 20.

IV. Discussion of the Results

The results obtained from the time-domain simulation studies for the system under investigations are summarized in Table II and analyzed as follows:

- The current setting of Relay (40) does not satisfy the coordination between the relay and GUEC. Therefore, to ensure such coordination, the relay reach is reduced to 5.71 and 6.56 Ω for Zones 1 and 2, respectively, as shown in Fig. 5. In the absence of the midpoint STATCOM, the new

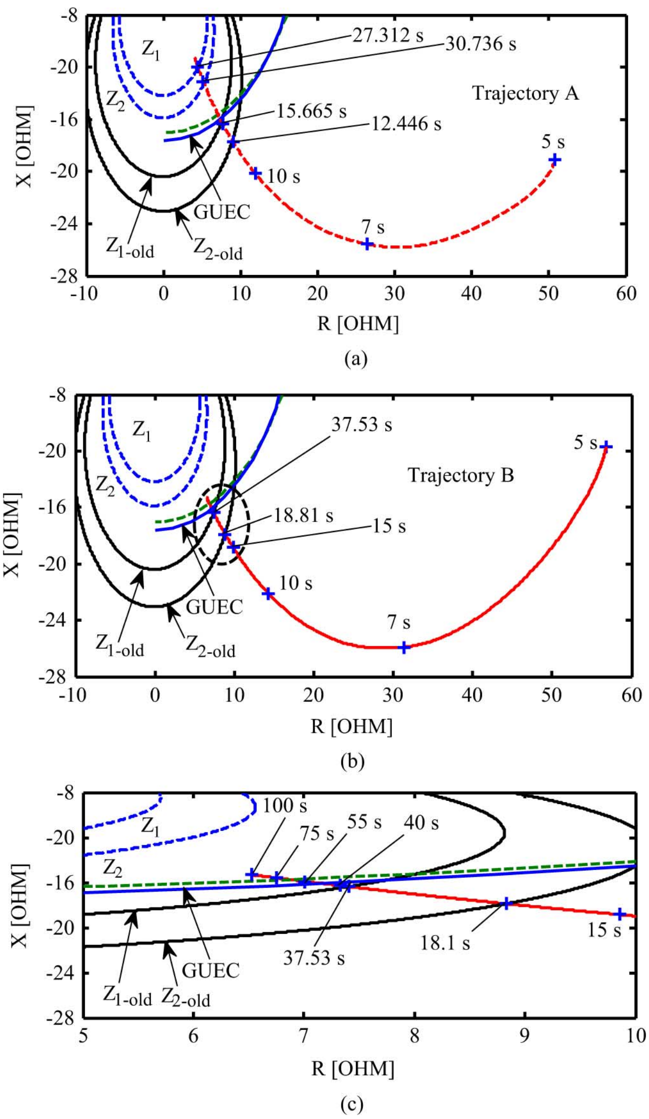

Fig. 21. Impedance trajectory measured by Relay (40) during Case 4: (a) without STATCOM total overview, (b) with STATCOM total overview, and (c) a zoom in on the trajectory after penetrating the relay characteristic.

relay setting satisfies the required coordination for all case studies as can be seen from Figs. 11(a), 14(a), and 18(a)

- In the presence of the midpoint STATCOM, the impedance trajectory seen by the relay takes a longer time to converge to a new steady-state value. This delay subjects the generator to undesirable longer lime operation in the leading VAR region as shown in Figs. 11(b), 14(b), 18(b), and 20. The nature of such an impact delay/underreach varies according to the generator loading and the LOE mode.
- At heavy generator loadings, the impact of the STATCOM on Relay (40) appears only in the form of delay time (delaying the UV supervising element and both Zones 1 and 2 elements) during all LOE modes. The maximum delay time is 9.55 s, during a partial LOE (($E_{F1} = 0.4$ p.u.) as shown in Fig. 14.
- At heavy generator loadings, the impact of the STATCOM extends to affect the healthy parallel generator by extending the overloading time of its armature and field windings. This is true for all LOE modes.
- At light generator loadings, the impact of the STATCOM appears in the form of a delay time in the operation of Relay (40) during complete LOE, while during a partial LOE, a UR phenomenon is detected.
- The worst impact of the STATCOM is the UR phenomenon where Relay (40) cannot detect an LOE condition unless it loses its coordination with (encroaches) the GUEC.

V. Conclusion

In this paper, investigations are carried out to explore the performance of generator LOE protection [Relay (40)] of a hydrogenerator power station with the presence of a midpoint STATCOM. The results of these investigations have shown that the midpoint STATCOM extremely affects the operation of Relay (40) and disturbs the coordination between the relay and the GUEC. The nature of such effects of time delay and underreach varies according to the generator loading and the LOE mode. It has been also shown that such an impact (delay/underreach) on Relay (40) permits undesirable longer time operations of a heavy loaded generator in the leading VAR region. Moreover, the impact of the midpoint STATCOM extends to include the healthy parallel generator during heavy loadings by subjecting it to longer overloading periods. These results highlight the need for the search of new methods to achieve better generator LOE protection when STATCOM controllers are in service. The authors are presently utilizing the support vector machines (SVMs) and adaptive neurofuzzy inference systems (ANFIS) classification techniques to enhance generator LOE protection. This will be the subject of a future paper.

Appendix

1) *Each Generator*:300 MVA, 23 kV, $\mathrm{RPFA} = 19.95^{\circ}$, $\mathbf{x}_{\mathrm{d}} =$ j 1.15 p.u., $\mathbf{x}_{\mathrm{q}} =$ j 0.75 p.u., $\mathbf{x}_{\mathrm{d}}^{\backslash} =$ j 0.314 p.u., $\mathrm{x}_{\mathrm{d}}^{\backslash\backslash} =$ j 0.25 p.u.
2) *Relay (40):* Original setting: $\mathrm{Z}_1 = 17.63\ \Omega$, $\mathrm{Z}_2 = 20.275\ \Omega$, Reduced setting: $\mathrm{Z}_1 = 5.71\ \Omega$, $\mathrm{Z}_2 = 6.56\ \Omega$, Z_1 delay time = 0.1 s, Z_2 delay time = 0.5 s, UV element = 0.87 p.u. with 0.9 s delay time, $\mathrm{R}_{\mathrm{C}} = 1600$, $\mathrm{R}_{\mathrm{V}} = 200$.
3) *GSU Transformer*: 300 MVA, 23 kV $\Delta/345$ kV Y_{g}, $x_{\mathrm{T}} =$ j 0.1 p.u.
4) *Transmission lines and equivalent system*345 kV, 300 km, $\mathrm{r}_{\mathrm{line}} = 0.037\,\Omega/\mathrm{km}$, $\mathrm{x}_{\mathrm{line}} = 0.367\,\Omega/\mathrm{km}$, $\mathrm{b}_{\mathrm{line}} = 4.518\times 10^{-6}\ \mathrm{S/km}$, $\mathrm{z}_{\mathrm{S1}} = 15\ \Omega$ at 85 °.
5) *STATCOM:* 12-Pulse, ±100 MVAR, coupling transformer (Y/y/d): 345/11/11 kV, $\mathrm{x}_T =$ j 0.1 p.u., $\mathrm{C} = 300\ \mu$F.

References

[1] *North Electric Reliability Corporation (NERC), Power Plant and Transmission System Protection Coordination*, Jul. 2010.
[2] F. A. Albasri, T. S. Sidhu, and R. K. Varma, "Impact of shunt-FACTS on distance protection of transmission lines," presented at the Power Syst. Conf., Clemson, SC, USA, Mar. 14–17, 2006.
[3] F. A. Albasri, T. S. Sidhu, and R. K. Varma, "Performance comparison of distance protection schemes for shunt-FACTS compensated transmission lines," *IEEE Trans. Power Del.*, vol. 22, no. 4, pp. 2116–2125, Oct. 2007.

[4] M. Elsamahy, S. O. Faried, and R. Gokaraju, "Impact of midpoint STATCOM on the coordination between generator distance phase backup protection and generator capability curves," presented at the IEEE Power Energy Soc. Gen. Meeting, Minneapolis, MN, USA, Jul. 25–29, 2010.

[5] M. Elsamahy, S. O. Faried, T. S. Sidhu, and R. Gokaraju, "Enhancement of the coordination between generator phase backup protection and generator capability curves in the presence of a midpoint STATCOM using support vector machines," *IEEE Trans. Power Del.*, vol. 26, no. 3, pp. 1841–1853, Jul. 2011.

[6] P. Kundur, *Power System Stability and Control*. New York: McGraw-Hill, 1994.

[7] *IEEE Guide for Operation and Maintenance of Hydro-Generators*, IEEE Standard 492, 1999.

[8] G. Benmouyal, "The impact of synchronous generators excitation supply on protection and relays," *Schweitzer Eng. Laboratories, Inc., 20070912.TP6281–01*, pp. 1–16, 2007. [Online]. Available: http://www.selinc.com/search/WebSearch.aspx?t=Gabriel%20Benmouyal&f=0

[9] D. Zlatanovici, P. Budulan, and R. Zlatanovici, "Assessment of hydrogenerators capacity to provide the system service of voltage control in the secondary band," presented at the IEEE Bologna Power Tech Conf., Bologna, Italy, Jun. 23–26, 2003.

[10] D. Sumina, A. Sala, and R. Malaric, "Determination of load angle for salient-pole synchronous machine," *Meas. Sci. Rev. J.*, vol. 10, no. 3 , pp. 89–96, 2010.

[11] G. R. Bérubé and L. M. Hajagos, "Coordination of under excitation limiters and loss of excitation relays with generator capability," presented at the IEEE Power Energy Soc. Gen. Meeting, Calgary, AB, Canada, Jul. 26–30, 2009.

[12] *Salient-Pole 50 Hz and 60 Hz Synchronous Generators and Generator/Motors for Hydraulic Turbine Applications Rated 5 MVA and Above*, IEEE Standard C50.12, 2005.

[13] *IEEE Recommended Practice for Excitation System Models for Power System Stability Studies*, IEEE Standard 421.5, 2005.

[14] D. Reimert, *Protective Relaying for Power Generation Systems*. Boca Raton, FL, USA: CRC, 2006.

[15] *IEEE Guide for AC Generator Protection*, IEEE Standard C37.102,, 2006.

[16] N. G. Hingorani and L. Gyugyi, *Understanding FACTS Concepts and Technology of Flexible AC Transmission Systems*. New York, USA: Wiley, 1999.

[17] R. M. Mathur and R. K. Varma, *Thyristor-based FACTS Controllers for Electrical Transmission Systems*. Hoboken, NJ, USA: Wiley/IEEE, 2002.

[18] *"PSCAD/EMTDC User's Manual,"* Manitoba HVDC Res. Ctr., Winnipeg, MB, Canada, 2003.

Mohamed Elsamahy (S'09–M'11) received the B.Sc. and M.Sc. degrees in electrical engineering from the Military Technical College (M.T.C), Cairo, Egypt, in 1997 and 2003, respectively, and the Ph.D. degree in electrical engineering from the University of Saskatchewan, Saskatoon, SK, Canada, in 2011.

Currently, he is an Assistant Professor in the Department of Electrical Power and Energy, M.T.C. From 1998 to 2008, he was a Teaching and Research Assistant at the same college. His current research interests include power system protection, control, power system dynamics, and intelligent applications in power systems.

Dr. Elsamahy is a Registered Professional Engineer in the Province of Saskatchewan.

Sherif Omar Faried (S'88–M'88–SM'00) received the B.Sc. and M.Sc. degrees in electrical engineering from Ain Shams University, Cairo, Egypt, in 1979 and 1984, respectively, and the M.Sc. and Ph.D. degrees in electrical engineering from the University of Saskatchewan, Saskatoon, SK, Canada, in 1988 and 1993, respectively.

From 1979 to 1984, he was a Teaching and Research Assistant in the Department of Electrical Power and Machines, Ain Shams University. Currently, he is a Professor of Electrical Engineering in the Department of Electrical and Computer Engineering, University of Saskatchewan. His current research interests include power system dynamics, control, reliability, protection, and power quality.

Prof. Faried is a Registered Professional Engineer in the Province of Saskatchewan.

Tarlochan Sidhu (SM'94–F'04) received the B.E. (Hons.) degree in electrical engineering from the Punjabi University, Patiala, India, in 1979, and the M.Sc. and Ph.D. degrees in electrical engineering from the University of Saskatchewan, Saskatoon, SK, Canada, in 1985 and 1989, respectively.

Currently, he is Dean of Faculty of Engineering and Applied Science, University of Ontario Institute of Technology, Oshawa, ON, Canada. From 1990 to 2002, he was a Professor and Graduate Chair of the Department of Electrical and Computer Engineering, University of Saskatchewan. From 2002 to 2010, he was the Chair of the Department of Electrical and Computer Engineering and Professor and Hydro One Chair in Power Systems Engineering, University of Western Ontario, London, ON, Canada. He was also with the Regional Computer Center, Chandigarh, India; Punjab State Electricity Board, India; and Bell-Northern Research Ltd., Ottawa, ON, Canada. His areas of research interests include power system protection, monitoring, and control.

Dr. Sidhu is a Fellow of the Institution of Electrical Engineers of the U.K.; Fellow of the Institution of Engineers, India; a Professional Engineer registered in the Province of Ontario; and a Chartered Engineer in the U.K.